Complex-scaling approach to the decay of Bose-Einstein condensates

Peter Schlagheck and Tobias Paul

Institut für Theoretische Physik, Universität Regensburg, 93040 Regensburg, Germany

The mean-field dynamics of a Bose-Einstein condensate is studied in the presence of a microscopic trapping potential from which the condensate can escape via tunneling through finite barriers. We show that the method of complex scaling can be used to obtain a quantitative description of this decay process. A real-time propagation approach that is applied to the complex-scaled Gross-Pitaevskii equation allows us to calculate the chemical potentials and lifetimes of the metastably trapped Bose-Einstein condensate. The method is applied to a one-dimensional harmonic confinement potential combined with a Gaussian envelope, for which we compute the lowest symmetric and antisymmetric quasibound states of the condensate. A comparison with alternative approaches using absorbing boundary conditions as well as complex absorbing potentials shows good agreement.

I. INTRODUCTION

With the advent of optical lattices and "atom chips" [1], it became possible to probe the transport properties of a Bose-Einstein condensate in the mesoscopic regime. Experiments in this context include the observation of Bloch oscillations [2,3], the guided and free propagation of condensates through waveguide structures [4,5], the transport of condensates with "optical tweezers" [6], as well as the realization of Josephson junctions [7] and matter-wave interferometry [8], to mention just a few examples. Those experiments typically involve rather small trapping potentials, with length scales that can be of the order of a few microns. In such microscopic geometries, *decay* mechanisms of the condensate become a relevant issue. On the one hand, the condensed state is, at finite atom densities, subject to depletion, which is caused by the interaction with the thermal cloud and by three-body collisions. On the other hand, the condensate can escape from the trapping potential by tunneling through its barriers, if the chemical potential of the condensed atoms exceeds the background potential in the free space outside the trap. In that case, the self-consistent mean-field state of the condensate is no longer bound, but rather corresponds to a metastable "resonance" state, in a similar way as, e.g., doubly excited electronic states in the helium atom.

From the theoretical point of view, the problem of metastable states of Bose-Einstein condensates in such "open" trapping potentials was first approached by Moiseyev *et al.* in Ref. [9]. In this work, the mean-field dynamics of a condensate was studied in the presence of an isotropic harmonic confinement that is combined with a Gaussian envelope. Decaying states of the condensates were identified with self-consistent solutions of the stationary Gross-Pitaevskii equation at complex-valued chemical potentials, where complex absorbing potentials at the boundaries of the numerical grid were used to account for the escape of the condensate. As a result, a cross over from a decaying (resonance) state to a bound state of the condensate was found for a finite attractive interaction between the atoms.

The calculations of Ref. [9] were satisfactory from the quantitative point of view, but raised an important open question: How can "resonances," i.e., stationary states that describe the escape of population from an open confinement potential, be formally introduced in the framework of the nonlinear Gross-Pitaevskii equation? For linear systems, it is well known that this task is most conveniently accomplished by applying the method of "complex scaling" (or "complex rotation") [10–13]. This technique essentially amounts to the complex dilations $\mathbf{r} \mapsto \mathbf{r} e^{i\theta}$ and $-i\boldsymbol{\nabla} \mapsto -i\boldsymbol{\nabla} e^{-i\theta}$ of the position and momentum operators in the Hamiltonian that describes the quantum system under study. This transformation leads to a non-Hermitean Hamiltonian with a complex eigenvalue spectrum the continuous part of which is rotated to the lower half of the complex energy plane. Resonances, i.e., decaying states with eigenvalues corresponding to poles of the resolvent below the real energy axis, are thereby uncovered and can be calculated using standard diagonalization techniques for complex matrices. This approach is essentially *exact*, in the sense that no *a priori* approximations are introduced in the complex dilation procedure. Positions and widths of resonances can therefore be calculated with high precision by means of the complex scaling procedure [12,13].

Quite obviously, the extension of the method to the Gross-Pitaevskii equation is far from straightforward (see, e.g., the discussion in Ref. [14]). Indeed, the presence of the nonlinear term inhibits a direct formulation of complex scaling in terms of Green's functions or resolvents, which, for linear systems, provide the convenient link to the time-dependent decay problem. Furthermore, self-consistent solutions of the Gross-Pitaevskii equation are usually defined with respect to a given *normalization* of the condensate wave function ψ — which poses a conceptual problem for decaying states that are generally non-normalizable. An additional complication (which is quite severe from the numerical point of view, as we shall see later on) arises from the fact that the nonlinear term in the Gross-Pitaevskii equation contains the square modulus of ψ and is therefore a *nonanalytic* function of the condensate wave function.

This last difficulty was circumvented in a recently published approach by Moiseyev and Cederbaum [15]. In this work, the complex scaling transformation was applied to the exact microscopic many-particle dynamics of the bosonic

system, and a variational ansatz was used to derive from there a complex-scaled version of the Gross-Pitaevskii equation. This variational ansatz, however, was implicitly based on the assumption that the condensate wave function of the decaying state is entirely *real*, which effectively means that $|\psi(\mathbf{r})|^2$ can be replaced by the analytic term $\psi^2(\mathbf{r})$ in the Gross-Pitaevskii equation. Moiseyev and Cederbaum showed that chemical potentials and decay rates can be calculated from this complex nonlinear Schrödinger equation, whose behavior as a function of the interaction strength seems to be in qualitative agreement with the intuitive expectation.

Our ansatz in this paper is substantially different in the sense that we explicitly take into account the possibility of complex-valued resonance wave functions. As pointed out above, this introduces a major complication of the problem, due to the presence of the $|\psi(\mathbf{r})|^2$ term in the Gross-Pitaevskii equation. We solve this problem by formally defining separate dilations of ψ and its complex conjugate, and by performing explicit complex rotations of the wave function in the numerical implementation. Our approach is supported by calculations based on the "real," i.e., unscaled, Gross-Pitaevskii equation in presence of absorbing boundaries, with which we obtain good agreement.

The paper is organized as follows. In Sec. II A, we derive the relation between complex "resonance" solutions of the stationary Gross-Pitaevskii equation and the actual time-dependent decay process of the condensate. For the sake of simplicity, we restrict ourselves to the case of the one-dimensional mean-field dynamics of a Bose-Einstein condensate in a magnetic or optical waveguide. The complex scaling method and its application to the Gross-Pitaevskii equation is explained in Sec. II B, and details on the numerical implementation of the method are presented in Section II C. Section III contains the discussion of the numerical results that we obtain for a harmonic trapping potential with Gaussian envelopes.

II. COMPLEX SCALING OF THE GROSS-PITAEVSKII EQUATION

A. The time-dependent decay problem

We start from the one-dimensional time-dependent Gross-Pitaevskii equation

$$i\hbar \frac{\partial}{\partial \tilde{t}}\Psi(\tilde{x},\tilde{t}) = -\frac{\hbar^2}{2m}\frac{\partial^2}{\partial \tilde{x}^2}\Psi(\tilde{x},\tilde{t}) + V(\tilde{x})\Psi(\tilde{x},t)$$

$$+ 2a_s \hbar\, \omega_\perp |\Psi(\tilde{x},\tilde{t})|^2 \Psi(\tilde{x},\tilde{t}) \qquad (1)$$

which describes the mean-field dynamics of the condensate in presence of a tight cylindrical confinement with transverse frequency $\omega_\perp$. Here, m is the mass and a_s the s-wave scattering length of the atoms. For the sake of definiteness, we consider, as in Ref. [9], the open longitudinal potential

$$V(\tilde{x}) = \frac{1}{2}m\omega_0^2\tilde{x}^2\exp(-\tilde{\alpha}\tilde{x}^2), \qquad (2)$$

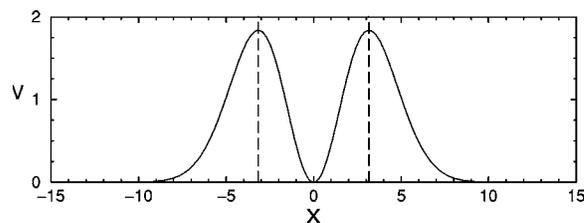which is shown in Fig. 1. Variants of Eq. (2) were exten-

FIG. 1. Effective longitudinal potential (3) for $\alpha=0.1$. The vertical dashed lines define the spatial region within which the wave function is normalized according to Eq. (7).

sively studied in the literature on resonances (e.g., Refs. [16–18]).

Since $V(\tilde{x})\rightarrow 0$ for $\tilde{x}\rightarrow\pm\infty$, the system does not exhibit any bound state. For not too large values of $\tilde{\alpha}$, however, the condensate can be temporarily stored within the potential well, from where it decays via tunneling through the barriers. In the linear case of noninteracting atoms ($a_s=0$), this decay process is described by resonance states $\Psi(\tilde{x},\tilde{t}) = \Psi(\tilde{x})\exp(-iE\tilde{t}/\hbar)$, where $\Psi(\tilde{x})$ satisfies the stationary Schrödinger equation for the complex energy $E=\mu-i\Gamma/2$ and exhibits outgoing (Siegert) boundary conditions [19] of the form $\Psi(\tilde{x})\rightarrow\Psi_0\exp(ik|x|)$ with $\mathrm{Re}(k)>0$ for $x\rightarrow\pm\infty$. An exponential decay $\propto\exp(-\Gamma\tilde{t}/\hbar)$ is therefore obtained for the atomic density inside the well if the system is initially prepared in such a resonance state. This is fundamentally different in presence of finite interaction ($a_s\neq 0$) where the tunnel coupling through the barriers explicitly depends, via the nonlinear term in the Gross-Pitaevskii equation, on the density $|\Psi(\tilde{x},\tilde{t})|^2$. As a consequence, the decay rate Γ varies during the time evolution of the condensate, which results in a nonexponential decay (see, e.g., Ref. [20]).

As long as the rate Γ characterizing the temporal variation of the density inside the well is comparatively small, the decay process can be approximately described by an adiabatic ansatz where the condensate is assumed to remain always in the energetically lowest (and most stable) resonance state associated with a given instantaneous density $|\Psi(\tilde{x},\tilde{t})|^2$. To this end, we introduce dimensionless variables which are formally obtained by setting $\hbar=m=\omega_0=1$. Specifically, we define the dimensionless potential

$$v(x) = V(a_0x)/\hbar\,\omega_0 = \frac{1}{2}x^2\exp(-\alpha x^2) \qquad (3)$$

with the dimensionless position $x=\tilde{x}/a_0$ and $\alpha=a_0^2\tilde{\alpha}$, where $a_0=\sqrt{\hbar/(m\omega_0)}$ is the oscillator length associated with the well (which would be of the order of several microns for typical experimental setups). We furthermore define, as a function of the effective interaction strength g, the dimensionless resonance state $\psi_g(x)$, together with its associated eigenvalue $E_g=\mu_g-i\Gamma_g/2$, as the solution of the stationary equation

$$H(\psi_g)\psi_g(x) = E_g\psi_g(x) \qquad (4)$$

with the dimensionless nonlinear Hamiltonian

$$H(\psi) = -\frac{1}{2}\frac{\partial^2}{\partial x^2} + v(x) + g|\psi(x)|^2. \qquad (5)$$

In addition to Eq. (4), we demand that ψ_g be normalized according to the condition

$$\mathcal{N}[\psi_g] \equiv \int_{-\infty}^{\infty} |\psi_g(x)|^2 w(x) dx = 1, \qquad (6)$$

where the weight function $w(x)$ measures the population inside the well. We shall use $w(x) = \theta(x_\alpha - x)\theta(x + x_\alpha)$ in the following, i.e.,

$$\mathcal{N}[\psi_g] = \int_{-x_\alpha}^{x_\alpha} |\psi_g(x)|^2 dx, \qquad (7)$$

where $x_\alpha = 1/\sqrt{\alpha}$ corresponds to the maximum of the barrier. We remark that the numerical results presented in Sec. III do not sensitively depend on the particular choice of x_α.

A further requirement that one should impose are outgoing boundary conditions for the wave function. Due to the self-consistent nonlinear term in the Gross-Pitaevskii equation, however, this requirement cannot be formulated in the same explicit way as for the linear case [19]. Qualitatively, such outgoing boundary conditions imply that the local current density of $\psi_g(x)$ is directed away from the trapping potential, and that no additional back reflections arise outside the support of $v(x)$. This means that the wave function evolves according to $\psi_g(x) \propto \exp[i\int^x k(x')dx']$, where the real part of the effective wave number $k(x)$ is positive (negative) for $x \gg x_\alpha$ ($x \ll -x_\alpha$) and varies smoothly with x to account for the variation of the self-consistent potential in Eq. (5). We shall assume that such a condition is met for the wave function ψ_g.

The adiabatic ansatz for $\Psi(\tilde{x},\tilde{t})$ is now formulated as

$$\Psi(\tilde{x},\tilde{t}) = \sqrt{\frac{N_0}{a_0}} \psi_{g(t)}(x)\exp\left(-i\int_0^t E_{g(t')}dt'\right) \qquad (8)$$

with $x \equiv \tilde{x}/a_0$ and $t \equiv \omega_0\tilde{t}$, where the effective time-dependent interaction strength is given by

$$g(t) = 2\frac{a_s}{a_0}\frac{\omega_\perp}{\omega_0}N(t). \qquad (9)$$

$N(t)$ is the time-dependent population inside the well and decays according to the equation

$$\frac{dN}{dt} = -\Gamma_{g(t)}N(t) \qquad (10)$$

with the initial condition $N(0) = N_0$, which is formally solved yielding

$$N(t) = N_0\exp\left(-\int_0^t \Gamma_{g(t')}dt'\right). \qquad (11)$$

As can be straightforwardly verified, $\Psi(\tilde{x},\tilde{t})$ satisfies the time-dependent Gross-Pitaevskii equation (1) as long as the temporal variation of $\psi_{g(\omega_0 t')}(\tilde{x}/a_0)$ (which is proportional to Γ_g) can be neglected in Eq. (1). We thereby obtain

$$\int_{-\infty}^{\infty} |\Psi(\tilde{x},\tilde{t})|^2 w(\tilde{x}/a_0)d\tilde{x} = N(\omega_0\tilde{t}). \qquad (12)$$

The full characterization of the time-dependent decay process within this adiabatic picture therefore requires to calculate the resonance states ψ_g and their complex energies E_g within the range $0 < g < g(0)$ for $a_s > 0$, and within $g(0) < g < 0$ for $a_s < 0$. We shall show now that this aim can be achieved with the method of complex scaling. To simplify the discussion, we shall drop the index g (i.e., $\psi \equiv \psi_g$ and $E \equiv E_g$) and consider $\alpha = 0.1$ in the following.

B. The complex scaling transformation

1. Linear case

Our aim is now to calculate the resonance states for the nonlinear Gross-Pitaevskii equation — i.e., the solutions of

$$H(\psi)\psi(x) = E\psi(x), \qquad (13)$$

with

$$H(\psi) = H_0 + g|\psi(x)|^2, \qquad (14)$$

$$H_0 = -\frac{1}{2}\frac{\partial^2}{\partial x^2} + v(x), \qquad (15)$$

that exhibit outgoing boundary conditions and are normalized according to

$$\int_{-x_\alpha}^{x_\alpha} |\psi(x)|^2 dx = 1. \qquad (16)$$

For the linear case, i.e., in the absence of interaction ($g = 0$), this aim can be straightforwardly achieved by the method of complex dilation. This operation is formally defined by the linear mapping

$$\psi(x) \mapsto \psi^{(\theta)}(x) \equiv R_\theta\psi(x) = e^{i\theta/2}\psi(xe^{i\theta}) \qquad (17)$$

which effectively amounts to a nontrivial scaling of the configuration space by the complex factor $\exp(i\theta)$. Applying this transformation to the stationary Schrödinger equation (13) (for $g = 0$) yields

$$H_0^{(\theta)}\psi^{(\theta)}(x) = E\psi^{(\theta)}(x), \qquad (18)$$

where

$$H_0^{(\theta)} \equiv R_\theta H_0 R_\theta^{-1} = -\frac{1}{2}e^{-2i\theta}\frac{\partial^2}{\partial x^2} + v(xe^{i\theta}) \qquad (19)$$

represents the (non-Hermitean) complex scaled Hamiltonian.

The spectral properties of the complex Schrödinger equation (18) are widely discussed in the literature on complex scaling [10–13]. While all eigenstates of the real equation (13) will formally solve also Eq. (18) after the transformation, their normalizability properties might change under the operation (17): Bound states of $v(x)$ (which are absent in our particular case) fall off sufficiently rapidly with increasing $|x|$, such that they remain normalizable under complex dilation (as long as $|\theta| < \pi/4$). This is, however, not true for
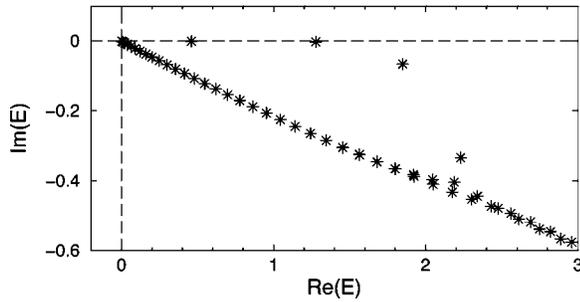
FIG. 2. Spectrum of the complex scaled Hamiltonian (19) for $\alpha=0.1$. The stars represent the complex eigenvalues of $H_0^{(\theta)}$ for $\theta=0.1$, which were calculated with a grid basis covering the range $-100\leqslant x \leqslant 100$. Four resonances are fully uncovered at this value of the rotation angle.

continuum states, which turn into wave functions that exponentially diverge for $|x|\rightarrow\infty$. For compensation, a "new" continuum of asymptotically oscillatory states arises in the rotated system, with eigenvalues along the axis $E=\epsilon e^{-2i\theta}$ with real ϵ.

The rotation of the continuum axis uncovers the spectral resonances of the system, which correspond to the poles of the analytical continuation of the Green function $G=(E-H_0+i\delta)^{-1}$ to the lower half part of the complex energy plane. Those resonances turn into discrete complex eigenvalues $E_n=\mu_n-i\Gamma_n/2$ under complex dilation and are represented by normalizable eigenfunctions $\psi_n^{(\theta)}(x)$ that can be straightforwardly calculated by diagonalizing $H_0^{(\theta)}$ in any numerical basis. This is illustrated in Fig. 2 which shows the spectrum of the rotated Hamiltonian (19) for $\theta=0.1$. In addition to "continuum" of levels along $E=\epsilon e^{-2i\theta}$ (which appears as discretized due to the finite basis), four major resonances can be identified below the real axis. Starting with an initial state that is very close to one of the resonances (i.e., which has, in the complex rotated system, a macroscopic overlap with the associated wave function $\psi_n^{(\theta)}$) will therefore lead to a decay from the well with a rate that is given by the negative imaginary part Γ_n of the corresponding eigenvalue.

2. Nonlinear case

In the nonlinear case, a major complication arises from the fact that the interaction-induced contribution $g|\psi(x)|^2$ to the Hamiltonian (14) is nonanalytic in ψ. To avoid this complication, it is tempting to make, in a first approach, the replacement

$$|\psi(x)|^2 \mapsto \psi^2(x) \tag{20}$$

in Eq. (14), i.e., to consider the analytic nonlinear Schrödinger equation

$$\widetilde{H}(\psi)\psi(x) = E\psi(x) \tag{21}$$

with

$$\widetilde{H} = H_0 + g[\psi(x)]^2. \tag{22}$$

Applying the complex scaling transformation (17) to Eq. (21) yields

$$\widetilde{H}^{(\theta)}(\psi)\psi^{(\theta)}(x) = E\psi^{(\theta)}(x) \tag{23}$$

with

$$\widetilde{H}^{(\theta)}(\psi) = H_0^{(\theta)} + g_\theta[\psi^{(\theta)}(x)]^2 \tag{24}$$

and $H_0^{(\theta)}$ being defined as in Eq. (19). Here the effective interaction strength is transformed according to

$$g \mapsto g_\theta = g e^{-i\theta} \tag{25}$$

in order to compensate the scaling prefactor $e^{i\theta/2}$ in Eq. (17). This additional scaling reflects the fact that g implicitly contains information about the norm of the wave function [see Eq. (9)].

The above approach yields meaningful results (i.e., results that are related to the actual time-dependent decay process of the condensate) only if the wave function $\psi(x)$ to be calculated in Eq. (4) is known to be *entirely real*. In general, this is not the case for unbound resonance states, which typically exhibit outgoing boundary conditions [i.e., $\psi(x) \propto \exp(ik|x|)$ for $|x|\rightarrow\infty$] and are therefore intrinsically complex. For such states, the replacement (20) represents a major modification of the problem, and the attempt to compute the decay behavior of the condensate by means of Eqs. (23)–(25) (which, in effect, were also used in Ref. [15]) would lead to a prediction that is not expected to be in agreement with alternative approaches based, e.g., on real-time propagation of the Gross-Pitaevskii equation in presence of complex absorbing potentials.

To account for the fact that ψ is complex valued, we formally introduce a second analytic wave function $\overline{\psi}$ which coincides with the complex conjugate of ψ on the real axis, i.e.,

$$\overline{\psi}(x) \equiv \psi^*(x) \quad \text{for real } x. \tag{26}$$

The complex scaling transformation is now defined for $\overline{\psi}$ in the same way as for ψ,

$$\overline{\psi}(x) \mapsto \overline{\psi}^{(\theta)}(x) \equiv R_\theta\overline{\psi}(x) = e^{i\theta/2}\overline{\psi}(xe^{i\theta}) \tag{27}$$

with R_θ the dilation operator. The analytic continuation of the stationary Gross-Pitaevskii equation to the complex domain then yields

$$H^{(\theta)}(\psi)\psi^{(\theta)}(x) = E\psi^{(\theta)}(x), \tag{28}$$

where the complex scaled Hamiltonian is given by

$$H^{(\theta)}(\psi) = H_0^{(\theta)} + g_\theta\overline{\psi}^{(\theta)}(x)\psi^{(\theta)}(x) \tag{29}$$

with $g_\theta = g e^{-i\theta}$. Note that $\overline{\psi}^{(\theta)}(x)$ is, in general, *not* identical to $[\psi^{(\theta)}]^*(x)$, the complex conjugate of $\psi^{(\theta)}$. It can, however, be obtained from $\psi^{(\theta)}$ via the relation

$$\overline{\psi}^{(\theta)}(x) = R_\theta(\overline{R_{-\theta}\psi^{(\theta)}})(x). \tag{30}$$

For weak or moderate nonlinearities (i.e., with g being of the order of unity or smaller), the spectrum of self-consistent

solutions of the complex scaled Gross-Pitaevskii Hamiltonian (29) can be assumend to be not much different from the linear case shown in Fig. 2: in addition to the continuum, a few quasibound resonance levels are expected to arise below the real energy axis. In the context of the actual time-dependent decay process of the condensate, we are mainly interested in the energetically *lowest* resonance, i.e., the one with the lowest real part μ of the complex eigenenergy $E = \mu - i\Gamma/2$ (which would adiabatically evolve into the self-consistent ground state of the potential well if the barrier height was raised to infinity). We shall explain now how the eigenfunction associated with this lowest resonance can be numerically calculated.

C. Numerical calculation of the resonance state

Our approach is based on the assumption that the lowest resonance state exhibits a decay rate that is not much larger than the decay rate of the lowest numerical continuum states. This is indeed true in the linear case, for the spectrum that is shown in Fig. 2: the width of the lowest resonance is found to be $\Gamma/2 \simeq 10^{-6}$, while the energetically lowest "continuum" state obtained from the numerical diagonalization (using a grid that covers the spatial range $-100 \leqslant x \leqslant 100$) decays with the rate $\Gamma/2 \sim 10^{-4}$. This observation suggests a real-time propagation approach to calculate the lowest resonance state. We start from a good initial approximation $\psi_0^{(\theta)}(x)$ for the resonant state (e.g., the harmonic eigenstate in the well), and numerically propagate $\psi^{(\theta)}$ under the time-dependent Gross-Pitaevskii equation

$$i\frac{\partial}{\partial\tau}\psi_\tau^{(\theta)}(x) = H^{(\theta)}(\psi_\tau)\psi_\tau^{(\theta)}(x) \qquad (31)$$

in the rotated system (τ is here a fictitious numerical "time" parameter, which is unrelated to the physical propagation time t in the actual decay process). In the above linear case, this propagation is guaranteed to converge towards the eigenstate with the lowest decay rate.

This approach works also for the nonlinear case, but requires some nontrivial modifications there. On the one hand, the self-consistent eigenstates and eigenenergies of the Gross-Pitaevskii equation are defined with respect to a given normalization of the wave function. A rescaling of $\psi^{(\theta)}$ according to the condition (16) is therefore required after each propagation step under Eq. (31). On the other hand, $\overline{\psi}_\tau^{(\theta)}(x)$ needs to be calculated from $\psi_\tau^{(\theta)}(x)$ in order to compute the nonlinear term in $H^{(\theta)}(\psi_\tau)$. In order to implement the prescription (30) which achieves this goal, the complex rotation (17) of the wave function needs to be explicitly performed. This operation, however, is known to be highly unstable [21] and requires great care in the numerical implementation.

In practice, two different basis sets are simultaneously used in order to numerically integrate Eq. (31). To perform the propagation, the rotated wavefunction is expanded in a grid basis, i.e.,

$$\psi_t^{(\theta)}(x) = \sum_{n=-n_{max}}^{n_{max}} C_n(t)\chi_n(x) \qquad (32)$$

with

$$\chi_n(x) = \begin{cases} 1/\Delta_x: & (n-1/2)\Delta_x < x < (n+1/2)\Delta_x \\ 0: & \text{otherwise,} \end{cases} \qquad (33)$$

where Δ_x is a suitable grid spacing. With the standard finite-difference approximation for the operator of the kinetic energy

$$-\frac{1}{2}\frac{\partial^2}{\partial x^2}\chi_n(x) \equiv -\frac{\chi_{n+1}(x) + \chi_{n-1}(x) - 2\chi_n(x)}{2\Delta_x^2}, \qquad (34)$$

we obtain a tridiagonal Hamiltonian matrix. This matrix is used to propagate the wavefunction according to the implicit scheme

$$\psi_{\tau+\delta\tau}^{(\theta)} = \left[1 + i\frac{\delta\tau}{2}H^{(\theta)}(\psi_\tau)\right]^{-1}\left[1 - i\frac{\delta\tau}{2}H^{(\theta)}(\psi_\tau)\right]\psi_\tau^{(\theta)}. \qquad (35)$$

The latter requires direct matrix-vector multiplications as well as the solution of linear systems of equations with tridiagonal matrices, which is efficiently performed by LR decompositions.

For the calculation of $\overline{\psi}^{(\theta)}$, a second, nonorthogonal basis set is introduced in terms of the analytic Gaussian functions

$$\phi_\nu(x) = \frac{1}{\sqrt{\sqrt{\pi}\sigma_\nu}}\exp\left(-\frac{(x-x_\nu)^2}{2\sigma_\nu^2}\right) \qquad (36)$$

for $-\nu_{max} \leqslant \nu \leqslant \nu_{max}$. The centers x_ν and widths σ_ν are chosen according to

$$x_\nu = \frac{\sinh(\nu\gamma)}{\sinh(\gamma)}\widetilde{\Delta}_x, \qquad (37)$$

for suitable parameters $\gamma, \widetilde{\Delta}_x > 0$, and

$$\sigma_\nu = x_{|\nu+1|} - x_{|\nu|}. \qquad (38)$$

The exponential increase of the widths σ_ν with $|\nu|$, which results from Eqs. (37) and (38), is required to ensure stable evaluation of linear combinations of ϕ_ν in the complex domain. ν_{max} is chosen such that the whole spatial range spanned by the grid basis is covered by the Gaussians.

From the overlap integrals $\mathcal{V}_{n,\nu} = \int\chi_n(x)\phi_\nu(x)dx$ and $\mathcal{I}_{\nu,\nu'} = \int\phi_\nu(x)\phi_{\nu'}(x)dx$, we can determine the expansion coefficients $D_{-\nu_{max}}\cdots D_{\nu_{max}}$ of $\psi_t^{(\theta)}(x)$ with respect to the Gaussian basis

$$\psi_t^{(\theta)}(x) = \sum_{\nu=-\nu_{max}}^{\nu_{max}} D_\nu(t)\phi_\nu(x). \qquad (39)$$

This involves again the solution of a linear system of equations, namely, $\Sigma_{\nu'}\mathcal{I}_{\nu,\nu'}D_{\nu'} = \Sigma_n\mathcal{V}_{n,\nu}C_n$, which is accomplished by the LR decomposition of the matrix $(\mathcal{I}_{\nu,\nu'})$ (the latter is effectively banded, due to the fact that the Gaussians fall off rapidly with increasing distance from their center). In a very similar way, we determine the rotation of the
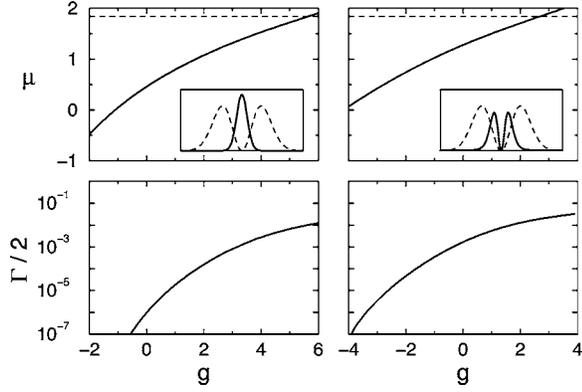
FIG. 3. Chemical potentials (upper panels) and decay rates (lower panels) of the lowest resonance state with even and odd parity (left and right column, respectively), as a function of the effective interaction strength g. The insets show the spatial density of the corresponding resonance states at $g=1$ (with the trapping potential indicated by dashed lines). Converged calculations of μ and Γ can be performed up to interaction strengths g where the chemical potential reaches the maximum barrier height of the potential, marked by the horizontal dashed lines in the upper panels. For $g < -1.1$, the lowest even state becomes stable, which manifests itself in a negative chemical potential and a vanishing decay rate.

wave function — i.e., the expansion of $(R_{-\theta}\psi_t^{(\theta)})(x)$ in the (unrotated) Gaussian basis (ϕ_ν) — by means of the overlap integrals $\mathcal{I}_{\nu,\nu'}$ and $\mathcal{J}_{\nu,\nu'} = \int \phi_\nu(xe^{i\theta})\phi_{\nu'}(x)dx$. Complex conjugation of the coefficients, the rotation R_θ, and the transformation back to the grid basis (χ_n) finally lead to the state vector $(\widetilde{C}_n)$ that is associated with $\overline{\psi}^{(\theta)}(x)$ [22].

We should note that the above method cannot properly reproduce $\overline{\psi}^{(\theta)}(x)$ far away from the center of the potential. This is due to the exponential increase of the widths and spacings of the Gaussians, which prevents a perfect representation of rapidly oscillating wave functions far away from the origin. We remark, however, that in the time-dependent Gross-Pitaevskii equation (31) $\overline{\psi}^{(\theta)}(x)$ is multiplied by the square of $\psi^{(\theta)}(x)$, and the term $(\overline{\psi}^{(\theta)}\psi^{(\theta)}\psi^{(\theta)})(x)$ decreases exponentially with $|x|$. Hence, apart from the special case of very large g and rapidly decaying resonance states, we obtain an approximation for $\overline{\psi}^{(\theta)}$ which is reasonably good in the relevant spatial regime to ensure stable convergence of our algorithm.

III. NUMERICAL RESULTS

A. Chemical potentials and decay rates

Figure 3 shows the chemical potentials and decay rates of the energetically lowest and of the first excited (solitonlike) quasibound state as a function of g (lower and upper solid curves, respectively) for $\alpha=0.1$. Due to the symmetry of the potential, both states can be calculated with the implicit propagation scheme described above, where the parity of the state is selected by the choice of the initial wavefunction. Typical parameters employed in the calculations are $\Delta_x \simeq 0.01$ for the grid spacing, $-100 \leqslant x \leqslant 100$ for the spatial range covered by the grid, $\theta = 0.05$ for the complex scaling

angle, and $\gamma \simeq 0.05$ for the parameter characterizing the exponential increase of the width of the Gaussians.

In the regime of small and moderate nonlinearities ($|g| \lesssim 1$), the numerical procedure described in the previous subsection is further optimized: To avoid time-consuming rotations of wave functions as best as possible, the renormalization of $\psi^{(\theta)}$ as well as the calculation of the nonlinear term in the Gross-Pitaevskii Hamiltonian are performed only every 100th propagation step according to Eq. (35). We verified, in any case, the convergence of the calculation by a criterion that is independent of the real-time propagation approach, namely, by the requirement that the norm of $\delta\psi^{(\theta)} = H^{(\theta)}(\psi)\psi^{(\theta)} - E\psi^{(\theta)}$ fall below a given precision limit. To obtain highly accurate results for the chemical potentials and the decay rates Γ, it is convenient to perform, for a given value of g, several calculations with different numerical grid spacings Δ_x (where the total extent of the grid is kept constant), and to extrapolate μ and Γ in the limit $\Delta_x \to 0$. In this way, rather low decay rates down to $\Gamma \simeq 10^{-7}$ can be reproduced.

Since no assumption about the sign of g was made in our approach, we can also calculate resonance (and bound) states for the case of *attractive* interaction. As we see in Fig. 3, the lowest even state of the trapping potential undergoes, for increasing attraction between the atoms, a transition from a resonance to a bound state, which is manifested by a negative chemical potential and a vanishing decay rate. In agreement with the calculation by Moiseyev *et al.* [9], which were performed for the same potential (3) with $\alpha = 0.2$, we find that this transition occurs at $g \simeq -1.1$.

For strong nonlinearities ($|g| > 1$), the renormalization of $\psi^{(\theta)}$ and the update of the nonlinear term need to be performed after each propagation step in order to ensure stable convergence of our approach. A further modification is introduced in the regime of large decay rates $\Gamma \sim 0.01$, i.e., where μ approaches the height of the potential barriers: To avoid unwanted convergence to energetically low continuum states (with decay rates $\Gamma \sim 10^{-4}$, see Sec. II B), we replace, in this regime, the real-time propagation approach by a propagation along a *complex* time path, given by $\tau = \tilde{\tau}e^{i\varphi}$ with real $\tilde{\tau}$ and $0 < \varphi < 2\theta$. A stationary solution ψ of the Gross-Pitaevskii equation will then evolve according to $|\psi_\tau^{(\theta)}(x)| = \exp[(\mu\varphi - \Gamma/2)\tilde{\tau}]|\psi_0^{(\theta)}(x)|$ for small φ, and quasibound states with finite μ will thereby be more strongly enhanced than low-energy continuum states close to the threshold. Indeed, we find that this modification allows converged calculations of resonances with chemical potentials close to the barrier height.

Table I shows a comparison of the chemical potentials and decay rates with the ones that are obtained from real-time propagation approaches based on the original (i.e., unrotated) Gross-Pitaevskii equation (4). In those calculations, the decay through the boundaries of the numerical grid is accounted for by absorbing boundary conditions [23,24] as well as by a complex absorbing potential of the form $V_{abs}(x) = -i(x/100)^{10}$ (for the spatial range $-100 \leqslant x \leqslant 100$). As in the complex scaling approach, the wave function was propagated by an implicit scheme such as (35) (now under the *real*, unscaled Gross-Pitaevskii Hamiltonian) and renor-

TABLE I. Chemical potentials and decay rates of the lowest quasibound state, calculated with the complex scaling (CS) approach and with real-time ropagation methods using absorbing boundary conditions (ABCs) and complex absorbing potentials (CAPs).

g	μ_{CS}	μ_{ABC}	μ_{CAP}	$\Gamma_{CS}/2$	$\Gamma_{ABC}/2$	$\Gamma_{CAP}/2$
0	0.4601	0.4602	0.4602	9.35×10^{-7}	9.55×10^{-7}	9.62×10^{-7}
1	0.7954	0.7955	0.7954	1.82×10^{-5}	1.81×10^{-5}	1.80×10^{-5}
2	1.0765	1.0773	1.0772	1.55×10^{-4}	1.56×10^{-4}	1.56×10^{-4}
3	1.3190	1.3193	1.3192	8.05×10^{-4}	8.04×10^{-4}	8.05×10^{-4}
4	1.5315	1.5313	1.5312	2.76×10^{-3}	2.75×10^{-3}	2.75×10^{-3}
5	1.7236	1.7230	1.7231	6.65×10^{-3}	6.66×10^{-3}	6.63×10^{-3}
6	1.9043	1.9034	1.9035	1.24×10^{-2}	1.23×10^{-2}	1.23×10^{-2}

malized after each step to satisfy the condition (7). The agreement between the three methods is reasonably good.

We should note, however, that strongly deviating values for Γ would generally be obtained if the resonance states were calculated according Eqs. (23), (24) under the assumption that the wave function ψ is entirely real. For $g=1$, e.g., the real-time propagation approach (35) using $\widetilde{H}^{(\theta)}$ [from Eq. (24)] instead of $H^{(\theta)}$ yields essentially the same chemical potential $\mu \simeq 0.795$, but a different decay rate $\Gamma/2 \simeq 5\times10^{-5}$. Also for $g=5$ we obtain $\Gamma/2 \simeq 1.6\times10^{-2}$ which considerably overestimates the actual rate $\Gamma/2 \simeq 6.7\times10^{-3}$. The above calculations based on $\widetilde{H}^{(\theta)}$ were performed under the slightly modified side condition $\int_{-x_\alpha}^{x_\alpha}[\psi(x)]^2 dx=1$, which would be consistent with Eq. (16) for purely real ψ [the propagation of $\psi^{(\theta)}$ under $\widetilde{H}^{(\theta)}$ does not seem to converge with the original side condition (16)].

B. Wave functions

While the chemical potentials μ and decay rates Γ are apparently well reproduced by the method of complex scaling, the wave functions $\psi(x)$ of the resonance states [defined according to Eq. (13), i.e., in the unrotated framework] can be calculated only in a limited spatial regime in the vicinity of the potential well. We attribute this to the exponential increase of the widths σ_ν and centers x_ν with $|\nu|$, which was introduced in order to ensure stable back rotation to the real domain. As already mentioned, this exponential scaling prevents a perfect representation of rapidly oscillating wavefunctions far away from the origin. For low and moderate nonlinearities ($g \lesssim 1$), we typically reproduce $\psi(x)$ up to distances of the order of $|x| \simeq 50$ from the center of the potential. This is illustrated in Fig. 4 where the wave functions of the even and odd resonance states at $g=1$ are plotted.

For large g, the spatial range in which ψ can be correctly reproduced becomes shorter. This is demonstrated in the upper panel of Fig. 5 which displays the wave function ψ_{CS} of the even resonance state at $g=5$ calculated with the complex scaling approach. In contrast to the actual resonance wave function (shown in the lower panel of Fig. 5), the density $|\psi_{CS}(x)|^2$ exhibits unphysical maxima near $|x| \simeq 25$ and de-
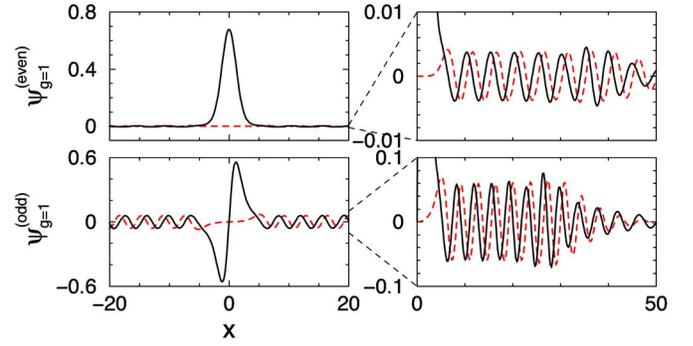

FIG. 4. (Color online) Wave functions of the even and odd resonance states at $g=1$ (upper and lower panels, respectively; solid lines: real part; dashed lines: imaginary part). The wave functions were calculated for the parameters $\gamma=0.05$ and $\widetilde{\Delta}_x=0.1$ of the Gaussian basis set [see Eq. (37)]. The magnifications in the right panels show that the outgoing tails of the wave functions are faithfully reproduced till $x \simeq 30$.

creases rapidly for larger $|x|$. We believe that those features arise due to the imperfect computation of the complex conjugate function $\overline{\psi}^{(\theta)}(x)$ by means of explicit rotations within the Gaussian basis set. It should be noted, however, that the values for μ and $\Gamma/2$ that are extracted from this wave function are nevertheless in good agreement with the chemical potentials and decay rates calculated with alternative methods at $g=5$ (see Table I).

Let us finally remark that from a formal point of view, even the "true" resonance wave function cannot be defined
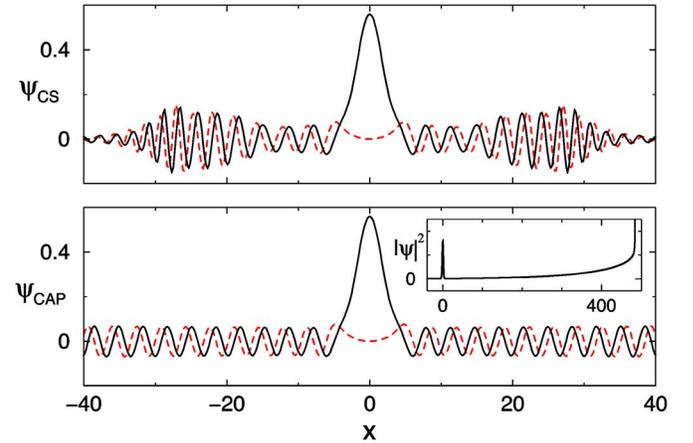

FIG. 5. (Color online) Wave function of the even resonance state at $g=5$ (solid line: real part; dashed line: imaginary part), calculated with the complex scaling method (upper panel) and with a real-time propagation approach using complex absorbing potentials (lower panel). The comparison shows that the complex scaling approach fails to correctly reproduce the resonance wave function for $|x| > 15$, even though the chemical potential and the decay rate are in agreement for both methods (see Table I). The insert in the lower panel displays the density of the resonance state continued till $x=500$, the tail of which was computed by integrating the free one-dimensional Gross-Pitaevskii equation [with $v(x) \equiv 0$] with the complex effective chemical potential $\mu_{g=5} - i\Gamma_{g=5}/2$, starting from $\psi_{CAP}(x=10)$. A singularity of $|\psi|^2$ is encountered at $x \simeq 485$ where the density exceeds the critical value μ/g.
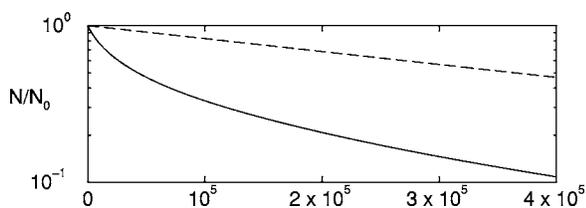
FIG. 6. Time-dependent decay of the condensate. Plotted is the number N of atoms inside the potential well as a function of time, with $N_0 \equiv N(t=0)$ such that $g=1$ initially. The dashed line shows the corresponding decay behavior of noninteracting atoms.

within an infinitely large spatial regime for $g > 0$: Due to the outgoing boundary conditions, the density $|\psi(x)|^2$ of the resonance wave function constantly increases with increasing $|x|$ outside the potential well, until it exceeds the critical value μ/g where the kinteic energy formally vanishes. Beyond that point, a rather sudden increase of the density towards infinity is encountered [25], which indicates that permanently time-dependent behavior would be expected for the actual decay process in that spatial regime. We should note, however, that the associated critical distance $|x| = x_c$ at which $|\psi(x)|^2$ equals μ/g is much larger than the spatial regime taken into account in our numerical calculations; for the even resonance state at $g=5$, e.g., we obtain $x_c \sim 500$ from $\mu \simeq 1.7$ and $\Gamma/2 \simeq 0.007$, while even larger critical distances ($x_c \sim 10^6$) would be expected for the more long-lived resonance states around $g=1$.

C. The time-dependent decay process

With the above method to calculate the decay rates of the resonance states for given nonlinearity strengths g, we are now in a position to predict the actual, real-time decay process of the condensate. As was derived in Sec. II A from the adiabatic approximation (8), the number of atoms in the potential well decreases with time according to

$$\frac{d}{dt}N(t) = -\Gamma_{g(t)}N(t), \qquad (40)$$

where $g(t)$ is proportional to $N(t)$ via Eq. (9):

$$g(t) = 2\frac{a_s}{a_0}\frac{\omega_\perp}{\omega_0}N(t). \qquad (41)$$

Multiplying Eq. (40) with the constant prefactors appearing in Eq. (41) yields the ordinary differential equation

$$\frac{d}{dt}g(t) = -\Gamma_{g(t)}g(t). \qquad (42)$$

This equation can be efficiently integrated, e.g., with a Runge-Kutta solver, provided the rates Γ_g are known in the range $0 \le g \le g(0)$.

Figure 6 shows the result of this integration for the case of repulsive interactions ($a_s > 0$). Here, the initial number of atoms $N(0)$ was assumed such that $g(0)=1$. The calculation was based on the decay rates $\Gamma_0, \Gamma_{0.1}, \ldots, \Gamma_1$ that were computed with the complex scaling method, and employed cubic

interpolation to obtain intermediate values for Γ_g. We clearly see that $N(t)$ decays initially according to a subexponential law, due to the fact that Γ decreases with decreasing g (a superexponential law would be encountered for attractive interaction). After about 10^5 time units, the exponential decay behavior of a noninteracting condensate (with decay rate $\Gamma_0 \simeq 2 \times 10^{-6}$) is recovered.

For comparison, we also performed a full time-dependent calculation of the decay process of the condensate. To this end, we first computed, using again Eq. (16) as side condition, the self-consistent ground state of the condensate at $g=1$ in the "closed" trapping potential

$$\bar{v}(x) = \begin{cases} v(x) : |x| < x_\alpha, \\ v(x_\alpha) : |x| > x_\alpha \end{cases}$$

with $x_\alpha = 1/\sqrt{\alpha}$, where the exterior part of $v(x)$ is replaced by a constant level corresponding to the height of the barriers. At $t=0$, $\bar{v}(x)$ was suddenly "opened," i.e., replaced by $v(x)$, and the wave function of the condensate's ground state was propagated under the time-dependent Gross-Pitaevskii equation at $g=1$, where absorbing boundary conditions were used to account for the decay through the boundaries of the numerical grid. The agreement between the two approaches is extremely good. At $t=4 \times 10^5$ for instance, when the surviving population of the condensate has decayed to $N(t) \simeq 0.1 N_0$, we find that the relative difference between the above propagation method and the integration of Eq. (42) (which takes much less CPU time, including the calculation of the decay rates Γ_g) is of the order of $\Delta N/N(t) \simeq 0.01$. This shows that the rates Γ_g obtained from the complex scaling approach are sufficiently precise to predict the time-dependent decay dynamics of the condensate.

IV. CONCLUSION

In summary, we have shown that the method of complex scaling can be used to calculate metastable mean-field states of Bose-Einstein condensates that are confined in trapping potentials with finite tunneling barriers. Our approach is based on the complex rotation $x \mapsto xe^{i\theta}$ of the Gross-Pitaevskii equation and employs, as key ingredients, separate dilations of the condensate wave function ψ and its conjugate $\bar{\psi}$, together with an additional scaling $g \mapsto ge^{-i\theta}$ of the interaction strength. A real-time propagation approach is used to calculate the lowest symmetric and antisymmetric quasi-bound states of the trapping potential and to determine the associated chemical potentials and decay rates. We find good agreement with alternative propagation methods that are based on the unrotated Gross-Pitaevskii equation and use absorbing boundary conditions as well as complex absorbing potentials to describe the decay.

Though only exemplified for the harmonic trap with Gaussian cutoffs, our method is sufficiently general to be applied to other trapping geometries, such as the double barrier potentials that are proposed in the context of resonant transport [24,26]. This is indeed confirmed in a recent study on the nonlinear Wannier-Stark problem, where the decay rates of the condensates were reproduced with the complex

scaling method [27]. The formalism presented here can, in addition, be straightforwardly generalized to describe decay processes in two- and three-dimensional geometries (which would naturally involve a higher numerical effort). Moreover, the framework of complex scaling seems also suited to be applied beyond the pure mean-field description of the condensate, e.g., in the context of fragmentation [28] and within the microscopic quantum dynamics approach [29]. We therefore expect that the complex scaling technique might develop into a useful tool to predict the storage time of condensates in microscopic trapping potentials, and to ad- dress the issue of resonances of the nonlinear Gross-Pitaevskii equation from the conceptual point of view.

[1] R. Folman, P. Krüger, D. Cassettari, B. Hessmo, T. Maier, and J. Schmiedmayer, Phys. Rev. Lett. **84**, 4749 (2000).

[2] B. P. Anderson and M. A. Kasevich, Science **282**, 1686 (1998).

[3] O. Morsch, J. H. Müller, M. Cristiani, D. Ciampini, and E. Arimondo, Phys. Rev. Lett. **87**, 140402 (2001).

[4] W. Hänsel, J. Reichel, P. Hommelhoff, and T. W. Hänsch, Phys. Rev. Lett. **86**, 608 (2001).

[5] H. Ott, J. Fortagh, G. Schlotterbeck, A. Grossmann, and C. Zimmermann, Phys. Rev. Lett. **87**, 230401 (2001).

[6] T. L. Gustavson, A. P. Chikkatur, A. E. Leanhardt, A. Görlitz, S. Gupta, D. E. Pritchard, and W. Ketterle, Phys. Rev. Lett. **88**, 020401 (2002).

[7] M. Albiez, R. Gati, J. Fölling, S. Hunsmann, M. Cristiani, and M. K. Oberthaler, Phys. Rev. Lett. **95**, 010402 (2005).

[8] T. Schumm, S. Hofferberth, L. M. Andersson, S. Wildermuth, S. Groth, I. Bar-Joseph, J. Schmiedmayer, and P. Krüger, Nat. Phys. **1**, 57 (2005).

[9] N. Moiseyev, L. D. Carr, B. A. Malomed, and Y. B. Band, J. Phys. B **37**, L193 (2004).

[10] E. Balslev and J. M. Combes, Commun. Math. Phys. **22**, 280 (1971).

[11] B. Simon, Ann. Math. **97**, 247 (1973).

[12] W. P. Reinhardt, Annu. Rev. Phys. Chem. **33**, 223 (1982).

[13] N. Moiseyev, Phys. Rep. **302**, 212 (1998).

[14] L. S. Cederbaum, F. Tarantelli, and P. Winkler, J. Phys. B **23**, L747 (1990).

[15] N. Moiseyev and L. S. Cederbaum, Phys. Rev. A **72**, 033605 (2005).

[16] N. Moiseyev, P. R. Certain, and F. Weinhold, Mol. Phys. **36**, 1613 (1978).

[17] M. Rittby, N. Elander, and E. Brändas, Phys. Rev. A **24**, 1636 (1981).

[18] H. J. Korsch and M. Glück, Eur. J. Phys. **23**, 413 (2002).

[19] A. J. F. Siegert, Phys. Rev. **56**, 750 (1939).

[20] S. Wimberger, R. Mannella, O. Morsch, E. Arimondo, A. Kolovsky, and A. Buchleitner, Phys. Rev. A **72**, 063610 (2005).

[21] A. Buchleitner, B. Grémaud, and D. Delande, J. Phys. B **27**, 2663 (1994).

[22] The rotation of $\psi^{(\theta)}$ back to the real domain is also employed for the determination of the factor by which the wave function has to be rescaled after each propagation step, in order to sat- isfy the normalization condition (16).

[23] T. Shibata, Phys. Rev. B **43**, 6760 (1991).

[24] T. Paul, K. Richter, and P. Schlagheck, Phys. Rev. Lett. **94**, 020404 (2005).

[25] This behavior can be straightforwardly reproduced by integrat- ing, with a Runge-Kutta solver, the ordinary differential equa- tion corresponding to the stationary Gross-Pitaevskii equation (13) in presence of a complex energy $E = \mu - i/2\Gamma$.

[26] I. Carusotto and G. C. La Rocca, Phys. Rev. Lett. **84**, 399 (1999); I. Carusotto, Phys. Rev. A **63**, 023610 (2001).

[27] S. Wimberger, P. Schlagheck, and R. Mannella, J. Phys. B **39**, 729 (2006).

[28] L. S. Cederbaum and A. I. Streltsov, Phys. Lett. A **318**, 564 (2003); Phys. Rev. A **70**, 023610 (2004).

[29] T. Köhler and K. Burnett, Phys. Rev. A **65**, 033601 (2002); T. Köhler, T. Gasenzer, and K. Burnett, *ibid.* **67**, 013601 (2003).